ISSN 2070-2051, Protection of Metals and Physical Chemistry of Surfaces, 2015, Vol. 51, No. 3, pp. 473–480. © Pleiades Publishing, Ltd., 2015.

PHYSICOCHEMICAL PROBLEMS OF MATERIALS PROTECTION

Corrosion Inhibition of Stainless Steel Type 316L in Hydrochloric Acid Solution using *p*-Aminoazobenzene Derivatives[1]

M. Abdallah[a, c], O. A. Hazazi[a], A. S. Fouda[b], and A. Abdel-Fatah[b]

[a]*Chemistry Department, Faculty of Applied Sciences, Umm Al-Qura University, Makkah, Saudi Arabia*

[b]*Chemistry Department, Faculty of Science, Mansoura University, Mansoura. 35516 Egypt*

[c]*Chemistry Department, Faculty of Science, Benha University, Benha, Egypt*

e-mail: metwally555@yahoo.com

Received January 30, 2014

Abstract—The inhibiting action of some *p*-aminoazobenzene derivatives towards the corrosion behavior of stainless steel type 316L in 3M HCl has been studied using weight loss, galvanostatic and potentiodynamic anodic polarization techniques. The inhibition efficiency of the investigated compounds was found to increase with increasing the concentration of inhibitor and with decreasing the temperature. The addition of KI to p-aminoazobenzene derivatives increased the inhibition efficiency due to synergistic effect. The presence of iodide ions in the solution stabilized the adsorption of these compounds on the steel surface and, therefore, improved the inhibition efficiency. Inhibition process was explained on the basis of adsorption of these compounds on the metal surface. The degree of surface coverage varied linearly with logarithm of inhibitor concentration fitting Temkin isotherm. Some thermodynamic parameters were calculated and discussed. It was found that, the *p*-aminoazobenzene derivatives provide a good protection to stainless steel against pitting corrosion.

DOI: 10.1134/S2070205115030028

1. INTRODUCTION

Stainless steel (type 316L) is frequently used as a construction material in various aggressive environments such as chemical plants, destination plants, waste water treatment plants and petroleum industry [1]. The present work was aimed to study of the corrosion of the metals specially SS type 316L which used in the industrial companies as the fertilizers companies and an example of these companies is Abu Zaabal company for Fertilizers and Chemicals (AZFC) which used SS type 316L in its phosphoric acid equipments (tanks, agitators, pumps, product lines). These equipments tired from the corrosion problem due to the contaminates exit in the mixture of the product as chlorides. The solution for this corrosion problem is to add organic or inorganic materials to inhibit the corrosion, and for that we study the corrosion of the AZFC stainless steel in hydrochloric acid. Stainless steel is resistant to corrosion due to the formation of a protective passive film that imparts corrosion resistance to its surface. However, chloride-containing acidic solution is aggressive to this film layer and results in severe pitting formation.

Organic compounds used as inhibitors act through a process of surface adsorption, so the efficiency of an inhibitor depends not only on the characteristics of the environment in which it acts, the nature of the metal surface and electrochemical potential at the interface, but also on the structure of the inhibitor itself, which includes the number of adsorption active centers in the molecule, their charge density, the molecule size, the mode of adsorption, the formation of metallic complexes and the projected area of the inhibitor on the metallic surface [2–13].

The inhibition mechanism of these organic compounds is mainly based on adsorption [14]. These compounds can adsorb on the steel surface blocking the active sites and thereby decreasing the corrosion rate. They control corrosion acting over the anodic or the cathodic surface or both.

The aim of the present work is to study the inhibitive effects some *p*-aminoazobenzene derivatives towards the corrosion of stainless steel type 316L in 3M HCl studied using different techniques.

2. EXPERIMENTAL METHODS

The composition of the stainless steel (type 316L) in wt % 0.02 C, 1.0 Si, 1.0 Mn, 0.2 Cu, 0.054 P, 0.02 S, 16 Cr, 11 Ni, and 3 Mo. Weight loss measurements were performed using coupons of the dimensions $2.0 \times 2.0 \times 2.0$ cm^3. For galvanostatic and potentiodynamic anodic polarization measurements, a cylindrical rod embedded in araldite with exposed surface of 0.3 cm^2 was used. The electrode was polished with different grades of emery paper, degreased with acetone and rinsed by distilled water. For galvanostatic experi-

[1] The article is published in the original.

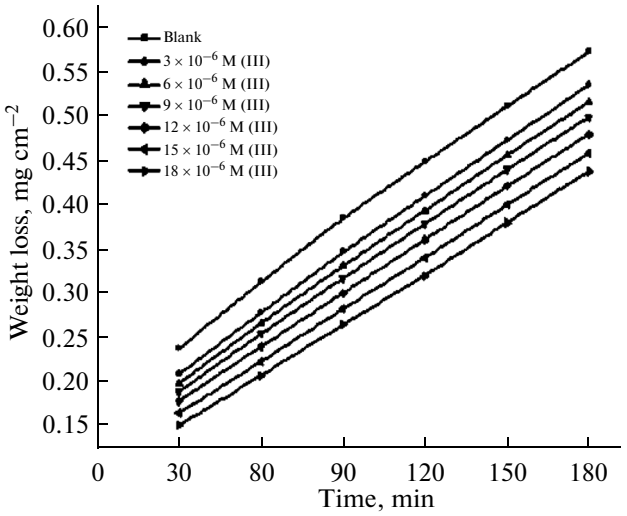

Fig. 1. Weight loss-time curves for SS type 316L dissolution in 3M HCl in presence and absence of different concentrations of inhibitor **III** at 30°C.

ments, the electrode was put under open circuit potential until stable potential was attained (about 30 min) and for potentiodynamic anodic polarization experiments, the electrode was held at hydrogen evolution potential for 10 min in order to get rid of any pre-immersion oxide film.

Weight loss measurements were carried out as described elsewhere [15]. The percentage inhibition efficiency and a parameter θ, which represents the part of the metal surface covered by the inhibitor molecules were calculated using the following equations:

$$IE = \left(1 - \frac{W_{add}}{W_{free}}\right) \times 100, \% \quad (1)$$

$$\theta = \left(1 - \frac{W_{add}}{W_{free}}\right), \quad (2)$$

where, W_{free} and W_{add} are the weight losses of SS type 316L coupon in free and inhibited acid solution, respectively.

Table 1. Inhibition efficiency at different concentrations of inhibitors as determined by weight loss method at 30°C and 60 min immersion

Inhibitor, M	*IE, %*			
	I	**II**	**III**	**IV**
3×10^{-6}	5.03	7.64	11.13	2.60
6×10^{-6}	9.37	12.45	14.77	7.06
9×10^{-6}	13.87	16.96	18.54	11.71
12×10^{-6}	19.17	20.37	23.26	15.73
15×10^{-6}	24.54	25.64	28.76	20.11
18×10^{-6}	28.94	29.80	33.64	24.58

Galvanostatic polarization studies were carried out using EG&G model 173 potentiostat/galvanostat. Three compartment cell with a saturated calomel reference electrode and a platinum foil auxiliary electrode was used. The percentage inhibition efficiency was calculated from corrosion current density values using the equation

$$IE = \left(1 - \frac{I_{add}}{I_{free}}\right), \% \quad (3)$$

where, I_{free} and I_{add} are the current densities in absence and presence of inhibitors, respectively.

Potentiodynamic anodic polarization technique was performed at a scanning rate of 1 mV/s using a Wenking potentioscan type POS 73 and the current density-potential curve were recorded on X-Y recorder type PL.3. The potentials were measured relative to a saturated calomel electrode (SCE) and the electrolytic cell is described elsewhere [16].

The structure of p-aminazobenzene derivatives is:

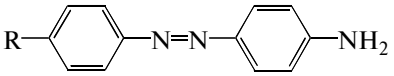

R=H, H_3C, H_3CO, O_2N

where R=H,CH_3, OCH_3 and NO_2 for compound **I**, **II**, **III**, and **IV**, respectively

3. RESULTS AND DISCUSSION

3.1. Weight Loss Measurements

Figure 1 represents the relation between time and weight losses of SS type 316L coupons in 3 M HCl solution devoid of and containing different concentrations of compound III as an example. Similar curves were also obtained for other three tested compounds. Inspection of this figure reveals that, the linear variation of weight loss with time in uninhibited and inhibited 3 M HCl solution indicates the absence of insoluble surface films during corrosion i.e. the inhibitors are first adsorbed on the metal surface and there after impede corrosion either by merely blocking the reaction sites (anodic and cathodic) or by altering the mechanism of the anodic and cathodic processes.

The calculated values of inhibition efficiencies obtained from weight loss are listed in Table 1. It is obvious that the *IE* increases with increasing the inhibitor concentration, whereas decreases in the following order: **III** > **II** > **I** > **IV**. This behavior will be discussed late.

3.2. Synergistic Effect of KI

All the experimental results have shown that the addition of iodide ions to the inhibitor containing solution increases the inhibitive efficiency. This behavior is attributed to the synergistic effect between

added iodide ions and *p*-aminoazobenzene derivatives.

The effect of KI on the inhibition efficiency of p-amino azobenzene derivatives has been studied using weight loss technique. The values of *IE* for specific concentration of KI (1×10^{-3} M) in presence of various concentrations of inhibitors are given in Table 2.

The extent of synergism between iodide ions and p-aminoazobenzene derivatives was evaluated using a parameter, S_θ obtained from the surface coverage θ of the anion and cation and both. Aramaki and Hackerman [17] calculated the synergism parameter S_θ, using the following equation:

$$S_\theta = (1 + \theta_{1+2})/(1 + \theta_{1+2}),$$

where $\theta_{1+2} = (\theta_1 + \theta_2) - (\theta_1\theta_2)$; θ_1 is the surface coverage of cation (protonated inhibitor); θ_2 is the surface coverage of anion I^-; θ'_{1+2} is the measured surface coverage by both the anion I^- and the cation (protonated inhibitor).

The calculated values of S_θ are given in Table 3. Inspection of Table 3 the values of S_θ are nearly equal to unity which suggests that the enhanced inhibition efficiencies caused by the addition of iodide ions to p-aminoazobenzene derivatives is due mainly to the synergistic effect.

The synergistic effect of iodide with *p*-aminoazobenzene derivatives may be due to the co-adsorption of halide ions and *p*-aminoazobenzene molecules which may be either competitive or co-operative [18]. In competitive adsorption the anion and cation are adsorbed at different sites on the metal surface. In co-operative adsorption, the anion is chemisorbed on the surface and the cation is adsorbed on the anion.

The co-adsorption of iodide ions on the surface which forms oriented dipole with their negative ends toward the solution, thus, increasing the adsorption of organic molecules [19]. Besides the nature of anions present in the acidic solutions, it plays a significant role in influencing the extent of adsorption. This is in turn may favor more adsorption of cations on the surface and resulting in more inhibition.

3.3. Effect of Temperature

The effect of temperature on the corrosion rate of SS type 316L in free acid and in presence of different inhibitors concentrations was studied in the temperature range of 30–50°C using weight loss measurements. Similar curves to Fig. 1 were obtained (not shown).

As the temperature increases, the rate of corrosion increases and hence the inhibition efficiency of the additives decreases. This is due to the desorption is aided by increasing the temperature. This behavior proves that the adsorption of inhibitors on SS type 316L surface occurs through physical adsorption.

Table 2. Inhibition efficiency at different concentrations of inhibitors in presence of 1×10^{-3} M of KI as determined from weight loss method at 30°C

Inhibitor, M	*IE*, %			
	I	**II**	**III**	**IV**
3×10^{-6}	41.25	43.44	46.03	37.15
6×10^{-6}	44.04	47.08	48.77	41.94
9×10^{-6}	45.68	51.32	52.80	46.37
12×10^{-6}	50.94	57.55	57.12	48.93
15×10^{-6}	54.39	61.00	61.3	53.19
18×10^{-6}	58.9	63.74	64.32	56.78

Table 3. Synergism parameter (S_θ) for different concentrations of all used inhibitors in 3M HCl in presence of 1×10^{-3} M of KI

Inhibitor concentration, C	S_θ			
	I	**II**	**III**	**IV**
3×10^{-6}	0.7866	0.7942	0.8010	0.7539
6×10^{-6}	0.7877	0.8046	0.8093	0.7787
9×10^{-6}	0.8163	0.8297	0.8394	0.8007
12×10^{-6}	0.8015	0.9124	0.8706	0.8026
15×10^{-6}	0.8049	0.9274	0.8953	0.8302
18×10^{-6}	0.8409	0.9418	0.9047	0.8487

The apparent activation energy E_a, the enthalpy of activation ΔH^* and entropy of activation ΔS^* for the corrosion of SS type 316L in 3 M HCl solutions in absence and presence of different concentrations of *p*-aminoazobenzene derivatives were calculated from Arrhenius-type equation [20]:

$$k = A\exp\left(\frac{-E_a}{RT}\right) \quad (5)$$

and transition state equation

$$k = \frac{RT}{Nh}\exp\left(\frac{\Delta S}{R}\right)\exp\left(\frac{-\Delta H}{RT}\right), \quad (6)$$

where k is the rate of metal dissolution, A is the frequency factor, N is Avogadro's number and R is the universal gas constant.

Figure 2 represents plot of $\log k$ against $1/T$ for SS type 316L in 3 M HCl solution in absence and presence of different concentrations of compound **III** as an example.

Similar curves were obtained for other compounds (not shown). Straight lines were obtained with slope equal to $-E_a/2.303R$. The values of E_a for the corrosion reaction in the absence and presence of different compounds was calculated and given in Table 2. On the other hand, Fig. 3 represents the plots of $\log(k/T)$ against $1/T$ for SS type 316L in 3 M HCl solution in

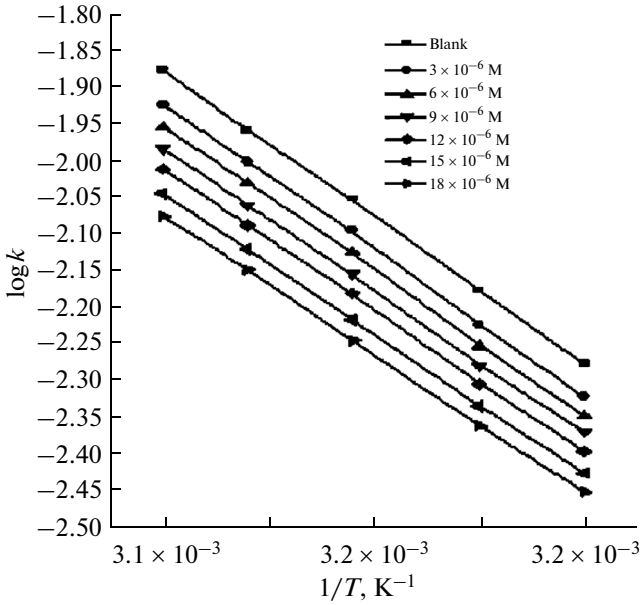

Fig. 2. $\log k - 1/T$ curve for SS type 316L dissolution in 3M HCl in presence and absence of different concentrations of compound

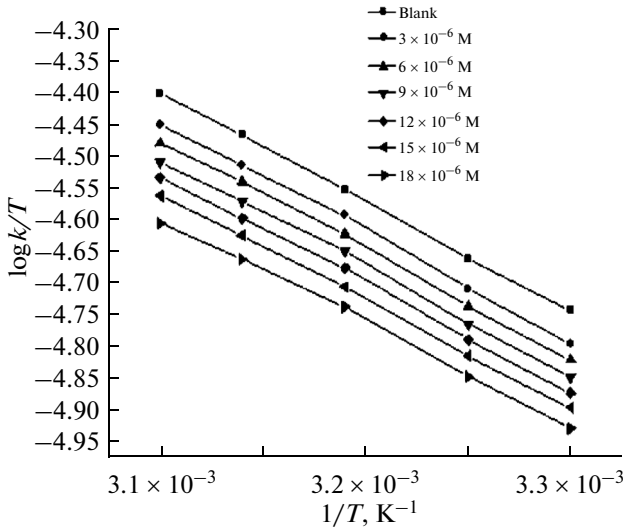

Fig. 3. $\log k/T - 1/T$ curve for SS type 316L dissolution in 3M HCl in presence and absence of different concentrations of compound **III**.

absence and presence of different concentrations of compound **III**. Similar curves obtained for other compounds (not shown). This relation gave straight lines with slope equals to $-\Delta H^*/2.303R$ and the intercept is $\log R/Nh + \Delta S^*/2.303R$. The obtained values of ΔH^* and ΔS^* are given in Table 4.

Inspection of Table 4 demonstrates that, the presence of *p*-aminoazobenzene derivatives increases the values of E_a indicating the adsorption of the inhibitor molecule on the metal surface. The values of E_a

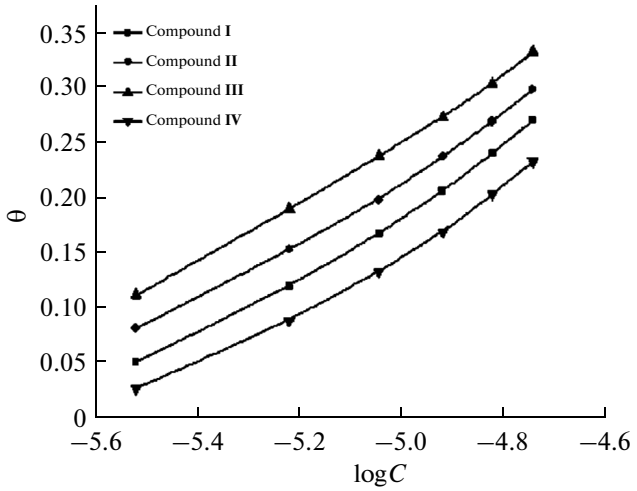

Fig. 4. Dependence of θ on the logarithm of inhibitor concentration at 30°C from weight loss technique.

increase with increasing the concentration of inhibitor. The obtained results suggested that *p*-aminoazobenzene derivatives inhibit the corrosion reaction by increasing its activation energy. The higher values of E_a indicate the physical adsorption of these compounds on SS surface. This could be done by adsorption on the stainless steel surface making a barrier for mass and charge transfer. However, such types of inhibitors perform a good inhibition at ordinary temperatures with considerable loss in the inhibition efficiency elevated temperatures.

The positive sign of ΔH^* reflect the endothermic nature of the steel dissolution process. Large and negative values of ΔS^* imply that the activated complex in the rate determining step represents an association rather than a dissociation takes place on going from reactants to the activated complex [21, 22].

3.4. Adsorption Isotherm

The experimental data for the tested additives have been applied to different adsorption isotherms. The best correlation among the experimental results obtained from the adsorption of additives on SS type 316L surface fit the Temkin adsorption isotherm.

A plot of surface coverage (θ) against $\log C$ (Fig. 4) approximately a straight line relationship in all cases was obtained. This suggests that the adsorption of p-aminoazobenzene derivatives on the steel surface follows Temkin isotherm. These results confirm the assumption that, these compounds are adsorbed on the metal surface through the protonated *N* atom or via the lone pair of electrons of nitrogen atoms. In addition to, the extent of inhibition is directly related to the performance of adsorption layer which is a sensitive function of the molecular structure.

Table 4. Activation parameters for the dissolution of SS type 316L in presence and absence of different concentrations of inhibitors in 3M HCl

Inhibitor	Concentration, M	Activation parameters		
		E_a, kJ mol^{-1}	ΔH^*, kJ mol^{-1}	ΔS^*, J mol^{-1} K^{-1}
Free acid (3 M HCl)	0	36.1013	31.0686	−190.7628
Compound **I**	3×10^{-6}	36.1366	31.3142	−186.1128
	6×10^{-6}	36.4921	31.9856	−184.0764
	9×10^{-6}	36.8267	32.5948	−183.3642
	12×10^{-6}	36.9892	32.7336	−181.7396
	15×10^{-6}	37.6284	32.9125	−180.5267
	18×10^{-6}	37.9946	33.2684	−180.2648
Compound **II**	3×10^{-6}	36.1427	31.3873	−185.7999
	6×10^{-6}	36.5107	32.0789	−183.9125
	9×10^{-6}	36.8946	32.6896	−183.1687
	12×10^{-6}	37.0082	32.7511	−181.6427
	15×10^{-6}	37.7913	32.9946	−180.3622
	18×10^{-6}	38.1067	33.3166	−180.1937
Compound **III**	3×10^{-6}	36.1541	31.4969	−185.7813
	6×10^{-6}	36.5758	32.2351	−183.7082
	9×10^{-6}	36.9277	32.7232	−183.1012
	12×10^{-6}	37.1361	32.7572	−181.5048
	15×10^{-6}	37.8734	33.0910	−180.1046
	18×10^{-6}	38.2155	33.3613	−180.1375
Compound **IV**	3×10^{-6}	36.1127	31.2681	−186.3476
	6×10^{-6}	36.4759	31.9264	−184.2866
	9×10^{-6}	36.8042	32.4927	−183.4827
	12×10^{-6}	36.9251	32.6658	−181.7894
	15×10^{-6}	37.5714	32.8973	−180.7436
	18×10^{-6}	37.8729	33.1866	−180.3729

3.5. Galvanostatic Polarization Studies

Figure 5 represents the anodic and cathodic polarization curves of SS type 316L in 3M HCl solutions devoid of and containing different concentrations of compound **IV** as an example of the studied additives. Similar curves were obtained for the other compounds (not shown).

An inspection of the curves in Fig. 5 reveals that the presence of the inhibitor decreases the corrosion rate (i-e) it shifted the anodic curves in the anodic direction and the cathodic curves in the cathodic direction this may be ascribed to the adsorption of the inhibitor molecules on the metal surface.

The electrochemical parameters such as, corrosion potential (E_{corr}), corrosion current density (I_{corr}), cathodic Tafel slope (β_c), anodic Tafel slope (β_a) and percentage inhibition efficiency were calculated and are given in Table 3. The corrosion current density (I_{corr}) and corrosion potential (E_{corr}) were determined by the intersection of the extrapolating anodic and cathodic Tafel lines, *IE* was calculated from Eq. (3) and β_a and β_c are the slopes of the anodic and cathodic Tafel lines.

Inspection of Table 5 reveals that, the increasing in the concentration of the additive show the following:

a—The Tafel lines are shifted to more positive and negative potential for anodic and cathodic processes, respectively, relative to the blank curve. This means that these compounds influence both cathodic and anodic processes. However, the data suggested that these compounds act mainly as mixed type inhibitors, but the cathode is more polarized when an external current was applied ($\beta_c > \beta_a$).

b—E_{corr} is nearly constant and the values of I_{corr} decreases indicating the inhibiting effect of these compounds.

c—The inhibition efficiencies of the four tested compounds by the polarization method decreases in the following order:

III > II > I > IV

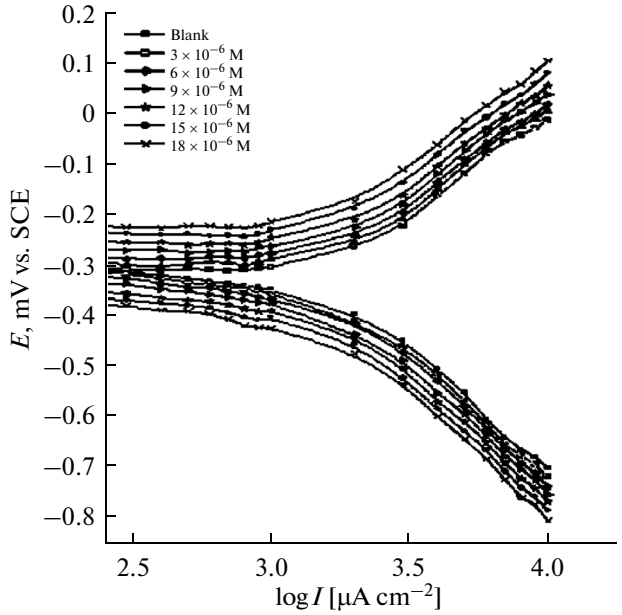

Fig. 5. Anodic and cathodic polarization curves for SS type 316L dissolution in 3M HCl in presence and absence of different concentrations of inhibitor **IV**.

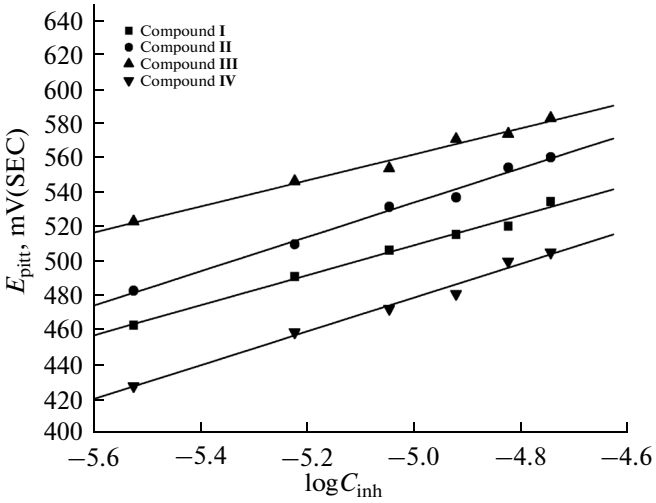

Fig. 6. The relationship between pitting potential of SS type 316L and logarithm various concentrations of the additives in presence of 0.1 M NaCl.

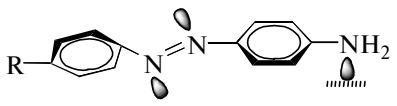

Fig. 7. Skeletal representation of the mode of adsorption of *p*-aminoazobenzene derivatives.

3.6. Pitting Corrosion

Potentiodynamic anodic polarization curves of SS type 316L were traced in solutions of 0.1 M NaCl (as a pitting corrosion agent) devoid of and containing different concentrations of *p*-aminoazobenzene derivatives at a scanning rate 1 mV/s.

The potential was swept from negative potential towards anodic direction up to the pitting potential, no any anodic oxidation peaks are observed in all anodic scan.

The pitting potential (E_{pitt}) was taken as the potential at which the current flowing, along the passive film increases suddenly to higher values, denoting the destruction of passive film and initiation of visible pits. The effect of addition of increasing concentration of *p*-aminoazobenzene derivatives on the values of pitting potential is illustrated in Fig. 6. This figure represents the relationship between E_{pitt} and logarithmic of molar concentration of additives. It is clear from this figure that, as the concentration of additives increases, the pitting potential shifted to more positive values in accordance with the following equation [23, 24].

$$E_{pitt} = a + b\log C_{inh}, \quad (7)$$

where a and b are constants depending on the type of additives used and the nature of the electrode. The positive shift of E_{pitt} indicates the increase resistance to pitting attack.

At one and the same inhibitor concentration the marked shift of potential in the noble direction (increased resistant to pitting corrosion) decreases in the following sequence:

III > II > I > IV

The different techniques used in this study gave the same order of inhibition efficiency but yielded different absolute values, probably due to the different experimental conditions.

3.7. Chemical Structure and Corrosion Inhibition

Inhibition of the SS (type 316L) corrosion in 3 M HCl solution by some *p*-aminoazobenzene derivatives using weight loss, galvanostatic polarization and potentiodynamic anodic polarization techniques can be explained on the basses of adsorption on the metal surface. The adsorption process was found to depend on the number of active sites in the molecules and their charge density, molecular size and stability of these derivatives in acidic solutions. The adsorption is assumed to take place mainly through the nitrogen atom of amino group (active centers). Transfer of lone pairs of electrons on the nitrogen to the surface to form coordinate type linkage is favored by the presence of vacant orbital in iron atom of low energy. Polar character of substituent in the changing part of the inhibitor molecule seems to have a prominent effect on the electron charge density of the molecule.

Skeletal representation of the mode of adsorption of the *p*-aminoazobenzene derivatives is shown in Fig. 7 and clearly indicates the adsorption centers.

Table 5. Electrochemical parameters obtained from galvanostatic polarization of SS type 316L in 3M HCl containing different concentrations of inhibitors at 30°C

Concn. M	$-E_{corr}$, mV	I_{corr}, m A cm^{-2}	β_a, mV dec^{-1}	β_b, mV dec^{-1}	0	*IE*, %
Compound **I**						
0	329	1.124	251	276	–	–
3×10^{-6}	323	1.066	267	318	0.05	5.16
6×10^{-6}	323	1.018	293	335	0.09	9.43
9×10^{-6}	328	0.974	331	340	0.13	13.30
12×10^{-6}	343	0.914	374	327	0.19	18.72
15×10^{-6}	336	0.853	382	336	0.24	24.14
18×10^{-6}	305	0.816	349	424	0.27	27.39
Compound **II**						
0	329	1.124	251	276	–	–
3×10^{-6}	323	1.042	262	326	0.07	7.27
6×10^{-6}	316	0.988	269	360	0.12	12.06
9×10^{-6}	324	0.941	297	367	0.16	16.21
12×10^{-6}	322	0.893	312	381	0.21	20.53
15×10^{-6}	305	0.847	307	427	0.25	24.63
18×10^{-6}	317	0.796	348	405	0.29	29.17
Compound **III**						
0	329	1.124	251	276	–	–
3×10^{-6}	326	1.004	248	311	0.11	10.63
6×10^{-6}	308	0.961	228	374	0.14	14.45
9×10^{-6}	323	0.916	291	362	0.18	18.4
12×10^{-6}	323	0.862	308	376	0.23	23.23
15×10^{-6}	307	0.805	306	402	0.28	28.35
18×10^{-6}	318	0.753	347	386	0.33	32.98
Compound **IV**						
0	329	1.124	251	276	–	–
3×10^{-6}	328	1.101	298	320	0.02	2.05
6×10^{-6}	336	1.044	326	310	0.07	7.10
9×10^{-6}	333	0.997	331	319	0.11	11.28
12×10^{-6}	339	0.961	376	336	0.14	14.49
15×10^{-6}	315	0.901	341	402	0.2	19.83
18×10^{-6}	315	0.855	360	427	0.24	23.97

From the above sequence of *IE*, it is clear that compound **III** is more efficient inhibitor for corrosion of SS type 316L in 3 M HCl solution. This is most probably due to the presence of methoxy group (OCH_3) which is one electron donating groups leading to increase the electron charge density on the molecule and hence increase in the inhibition efficiency of this compound. Compound **II** comes next to the compound **III** in spite of, it contains methyl group which is electron donating groups but less than methoxy groups. Compounds **I** come after compounds **II** due to it have H atom which is less donating than methyl groups. Compound **IV** are the least effective inhibitor in this sequence, because it has nitro groups which is withdrawing group.

4. CONCLUSIONS

1. *p*-aminoazobezene derivatives act as inhibitors for corrosion of SS type 316L in 3 M HCl solution.

2. The inhibition efficiency increases with increase in the concentration of these inhibitors but decreases with an increase in temperature.

3. The addition of KI to these compounds improves the values of inhibition efficiency due to synergistic effect.

4. The inhibition is due to the adsorption of the inhibitor molecule on the SS surface.

5. The adsorption of these compounds on the SS surface follows Temkin adsorption isotherm.

6. *p*-aminoazobenzene derivatives provide protection against pitting corrosion of SS type 316L in presence of chloride ions.

REFERENCES

1. Ait Albrimi, Y., Eddib, A., Douch, J., Berghoute, Y., Hamdani, M., and Souto, R.M., *Int. J. Electrochem. Soc.*, 2011, vol. 6, p. 4614.
2. Java Her Dashti, R., *Anti-Corros. Methods Mater.*, 2000, vol. 47, p. 30.
3. Elachouri, M., Infante, M.R., Izqnierdo, F., Kerti, S., Gonttaya, H.M., and Nciri, B., *Corros. Sci.*, 2001, vol. 43, p. 19.
4. Galal, A., Alta, N.F., and Hasan, M.H.S. Al., *Mater. Chem. Phys.*, 2005, vol. 89, p. 28.
5. Abdallah, M., *Corros. Sci.*, 2002, vol. 44, p. 717.
6. Abdallah, M., *Mater. Chem. Phys.*, 2003, vol. 82, p. 786.
7. Abdallah, M., Eletre, A.Y., Soliman, M.G., and Mabrouk, E.M., *Mater. Methods*, 2006, vol. 53, p. 118.
8. Hermas, A.A., Morad, M.S., and Wahdan, M.H., *J. Appl. Electrochem.*, 2004, vol. 34, p. 95.
9. Abdallah, M., Helal, E.A., and Fouda, A.S., *Corros. Sci.*, 2006, vol. 48, p. 1639.
10. Refaey, S.A.M., Taha, F., and Abd El-Malak, A.M., *Appl. Surf. Sci.*, 2004, vol. 236, p. 175.
11. Abdallah, M., Zaafarany, I., Khairou, K.S., and Ema, Y., *Chem. Technol. Fuels Oils*, 2012, vol. 48, p. 234
12. Abdallah, M., Asghar, B.H., Zaafarany, I., and Sobhi, M., *Prot. Met. Phys. Chem. Surf.*, 2013, vol. 49, p. 485.
13. Sobhi, M., Abdallah, M., and Khairou, K.S., *Monatsh. Chem.*, 2012, vol. 143, p. 1379.
14. Zadeh, A.R., Danaee, I., and Maddahy, M.H., *J. Mater. Sci. Technol.*, 2013, vol. 29, p. 884.
15. El-Etre, A.Y., *Corros. Sci.*, 2003, vol. 45, p. 2485.
16. El-Haleem, S.M., Abdel Fattah, A.A., and Tayor, W., *Res. Mech.*, 1985, vol. 15, p 87.
17. Aramki, K. and Hackerman, N., *J. Electrochem. Soc.*, 1969, vol. 116, p. 568.
18. Aramki, K., Hagiwara, M., and Nishihara, H., *Corros. Sci.*, 1987, vol. 27, p. 487.
19. Abdallah, M., Atwa, S.T., Salem, M.M., and Fouda, A.S., *Int. J. Electrochem. Soc.*, 2013, vol. 8, p. 10001.
20. Putilova, I., Balezin, S., Barannik, I.N., and Bioshop, V.P., in *Metallic Corrosion Inhibitors* Oxford: Pergamon, 1960, p. 196.
21. Marsh, J., *Advanced Organic Chemistry*, New Delhi: Wiley, 1988, 3d ed.
22. Abd El-Rehim, S.S., Ibrahim, M.A.M., and Khaled, K.F., *J. Appl. Electrochem.*, 1999, vol. 29, p. 593.
23. Abdallah, M. , Karane, S.A. Al., and Abdel Fattah, A.A., *Chem. Eng. Comm.*, 2010, vol. 197, p. 1446.
24. Abdallah, M., Al-Agez, M. and Fouda, A.S., *Int. J. Electrochem. Sci.*, 2009, vol. 4, p. 336.